Coverage, lateral order, and vibrations of atomic nitrogen on Ru(0001)

Cite as: J. Chem. Phys. **105**, 8944 (1996); https://doi.org/10.1063/1.472624
Submitted: 13 June 1996 • Accepted: 14 August 1996 • Published Online: 04 June 1998

H. Dietrich, K. Jacobi and G. Ertl

Coverage, lateral order, and vibrations of atomic nitrogen on Ru(0001)

H. Dietrich, K. Jacobi,[a] and G. Ertl
Fritz-Haber-Institut der Max-Planck-Gesellschaft, Faradayweg 4-6, D-14195 Berlin, Germany

(Received 13 June 1996; accepted 14 August 1996)

The N/Ru(0001) system was studied by thermal desorption spectroscopy (TDS), low-energy electron diffraction (LEED), and high-resolution electron energy-loss spectroscopy (HREELS). Atomic nitrogen was prepared by NH_3 decomposition at sample temperatures decreasing from 500 to 350 K during NH_3 exposure. A maximum N coverage of $\theta_N=0.38$ could thus be achieved. $\sqrt{3}$, split 2×2 and 2×2 LEED patterns were observed for decreasing θ_N. After NH_3 decomposition and before annealing the sample to a temperature above 400 K, the surface is composed of adsorbed N, H, and NH species. This composite layer exhibits a split $\sqrt{3}$ LEED pattern due to domains of size 4 with heavy walls. This phase decays through dissociation of NH leading to sharp first-order type desorption peaks of H_2 and N_2. From the weak intensity of the ν(Ru–NH) stretch mode it is concluded that NH is adsorbed at threefold-hollow sites. The energy of the ν(Ru–N) mode shifts from 70.5 to 75.5 meV when θ_N is increased from 0.25 to 0.38. © *1996 American Institute of Physics.* [S0021-9606(96)01643-1]

I. INTRODUCTION

The synthesis of ammonia from nitrogen and hydrogen on iron catalysts (the Haber–Bosch process) is an important industrial catalytic process. The underlying reaction mechanism consists of dissociative chemisorption of N_2 followed by hydrogenation of N on the surface.[1,2] Several groups have studied Ru catalysts which may replace Fe as the catalyst for ammonia synthesis.[3,4] The catalytic decomposition of ammonia on Ru surfaces is relevant in this context for a better understanding of the microscopic processes of ammonia synthesis. The interaction of ammonia with the clean and chemically modified Ru(0001) surface has previously been investigated by Parmeter *et al.*[5] and Zhou *et al.*[6]

Recently we have shown that the initial sticking coefficient for the dissociative adsorption of N_2 on Ru single crystal surfaces is only $(1\pm0.8)\times10^{-12}$ at room temperature.[7] In order to prepare high coverages of chemisorbed atomic nitrogen we used, therefore, the decomposition of NH_3 at temperatures above the desorption temperature of NH_3, a procedure which is well known.[8,9] The decomposition rate has been found to increase with increasing temperature. Egawa *et al.*[9] found a maximum decomposition rate at about 560 K while the maximum nitrogen coverage is obtained at lower temperatures. There exists however, contradictory results in the literature about the maximum coverage of the nitrogen ranging from $\theta_N=0.22$ (Ref. 10) to $\theta_N=0.47$.[8]

Here we use the decomposition of ammonia at sample temperatures well above its desorption temperature in order to prepare N coverages as high as possible. We will revise the maximum N coverage, which can be achieved, report on some new LEED patterns and show that, at lower preparation temperatures, NH is incorporated into the N layer.

II. EXPERIMENT

The experiments were carried out in an ultrahigh vacuum (UHV) apparatus with a base pressure of 1×10^{-11} mbar that was achieved by a pumping line free of oil consisting of a Ti sublimation pump, a turbomolecularpump with magnetic suspension (Leybold, NT340M), a drag pump (Balzers, TCP015), and a diaphragm pump. The apparatus consisted of two chambers; the upper chamber contained an argon ion gun, a quadrupole mass spectrometer, and a LEED optics. The lower chamber housed a high-resolution electron energy loss spectrometer (HREELS) for recording vibrational spectra. The two chambers were separated by a valve in order to keep the lower chamber at a pressure of 3×10^{-11} mbar during preparation of the sample in the upper chamber. The HREEL spectrometer was developed and mounted at the laboratory of Ibach.[11] HREEL spectra were taken at an angle of incidence of 60° with respect to the surface normal and in a specular geometry. The primary energy was 1.5 eV and the energy resolution was set to 3.4 meV. Typically, count rates in the elastic peak of about 3×10^5 counts/s were achieved.

The mass spectrometer was used to perform TDS measurements with a heating rate of 3 K s^{-1}. For this purpose the sample was positioned in front of a short stainless-steel tube with a diameter of about the sample size so that the ionizer of the mass spectrometer accepted predominantly molecules originating from the sample surface. During the TD measurements the mass spectrometer was pumped differentially by an ion getter pump. The signal for e/m ratios of 2, 14, 17, and 28 were recorded quasisimultaneously to follow the desorption of hydrogen, nitrogen, ammonia, and carbon monoxide. The cracking patterns of N_2 and CO differ with respect to mass 14 and, therefore, allowed to distinguish between CO and N_2 desorption. The Ru(0001) single crystal was mounted using W wires in narrow slits on the edges of the sample. The sample temperature was measured by a Ni–Cr/Ni thermocouple spot welded to the back side of the sample. Cleaning of the surface was achieved by repeated

[a]Author to whom all correspondence should be addressed.

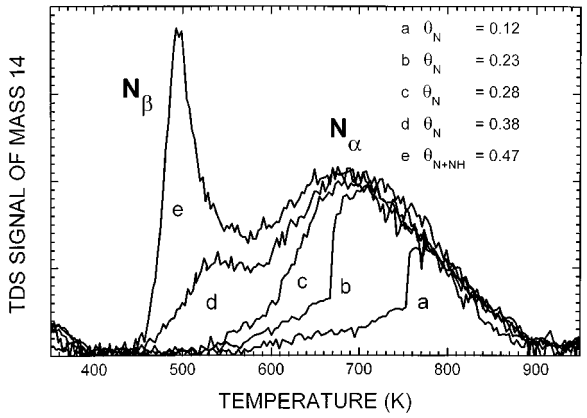

FIG. 1. TD spectra for a sequence of NH_3 exposures, (a) 500 L at 500 K, (b) 2500 L at 500 K, (c) 3500 L at 500 K, (d) exposure like in Fig. 2 followed by annealing to 520 K, (e) exposure like in Fig. 2. The pressure increase of mass 14 was recorded.

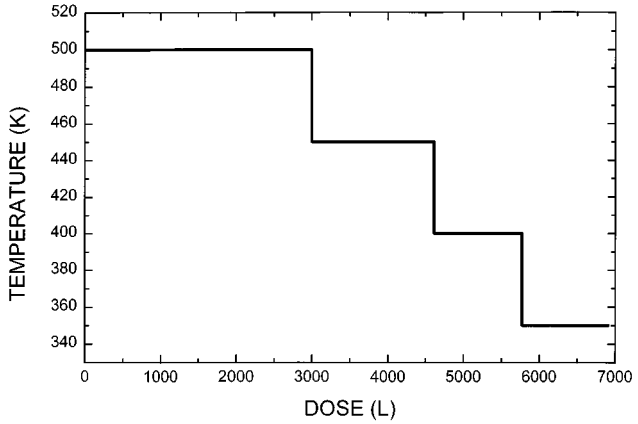

FIG. 2. Sample temperature during decomposition of NH_3 at a partial pressure of 5×10^{-6} mbar vs overall dose of NH_3 in units of langmuir (1 L$=1.33\times10^{-6}$ mbar×s).

cycles of sputtering and annealing to 1560 K. The cleanliness of the surface was verified by LEED and HREELS. The gas doses are given in units of langmuir (1 langmuir$=1.33\times10^{-6}$ mbar s). Coverages are given relative to the number of substrate surface atoms throughout the paper.

III. RESULTS

A. Thermal desorption spectroscopy

Figure 1 shows the TD spectra of mass 14 ($\hat{=}N_2$ desorption) for different ammonia exposures. Mass 14 was chosen to discriminate the nitrogen signal against desorption peaks resulting from a possible CO contamination. The values of the nitrogen coverages θ_N were determined by comparing the nitrogen TDS integrals of mass 28 with the TDS integrals of mass 28 of a saturated CO coverage at room temperature which results in $\theta_{CO}=0.56$.[12] The TD spectra a–c in Fig. 1 of the N_α state were prepared by dosing 500 L, 2500 L, and 3500 L of NH_3 at 5×10^{-6} mbar while the sample was kept at 500 K. These exposures resulted in total nitrogen coverages of $\theta_N=0.12$, $\theta_N=0.24$, and $\theta_N=0.28$. The shift in the peak temperature in the spectra a–c clearly represents a second-order desorption behavior as expected from the recombinative desorption of atomic nitrogen. Since the desorption of nitrogen in spectrum c sets-in at about 550 K, higher exposures (up to 6000 L) of NH_3 at 500 K did not result in a higher nitrogen coverage. In order to prepare higher coverages we chose the dosing procedure as sketched in Fig. 2. First we used the high decomposition rate at high sample temperatures. Keeping the ammonia pressure constant, we lowered then the sample temperature stepwise as indicated in Fig. 2. Directly after this dosing procedure the TD spectrum e of Fig. 1 was recorded. The total amount of desorbing nitrogen corresponds to $\theta_N=0.47$. Spectrum e exhibits a second, very sharp desorption peak at 500 K, the N_β state. While the N_α state was reported in the literature, this is the first time that the N_β state was observed. Assuming a first order process, an activation energy of 130 kJ/mol can be derived for the desorption of the N_β state. For spectrum d the NH_3 dose was the same as for spectrum e but the sample was annealed briefly to reduce the coverage. The nitrogen coverage was determined to $\theta_N=0.38$. At this dose also the N_α state is fully developed with a peak temperature of 680 K. The TD spectra of the N_α state are in very good agreement with published data[13] for which an activation energy of 190 kJ/mol was derived.

Figure 3 shows the TD spectra of mass 28 for the highest coverage displayed in Fig. 1 (spectrum e) and the TD spectrum of mass 2 which was recorded simultaneously. Note that the intensities in Fig. 3 are not corrected for the different ionization probabilities of N_2 (1.0) and H_2 (0.44). The high noise level is due to the relative short dwell time on mass 2 and the large background pressure. The hydrogen desorption sets-in at 380 K (H_α state) and at 460 K a second peak (H_β state) emerges almost in parallel with the N_β peak of the nitrogen desorption. The hydrogen desorption is completed at 540 K. The TD spectra for lower ammonia exposures

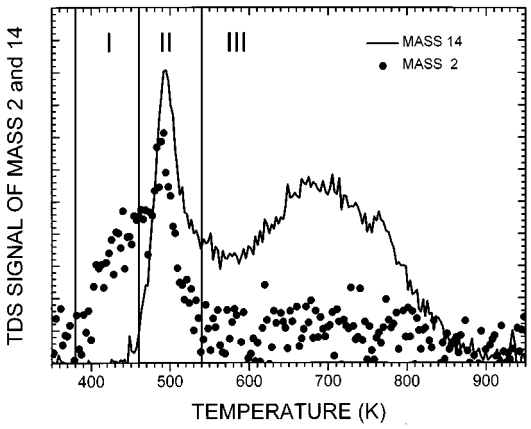

FIG. 3. TD spectra for the maximum exposure of NH_3 as shown in Fig. 2. The pressure increase of mass 14 and mass 2 was recorded simultaneously.

TABLE I. Coverages of hydrogen (θ_H), NH (θ_{NH}), and nitrogen (θ_N) on Ru(0001) following the decomposition of NH_3 according to the procedure given in Fig. 2 and annealing to the given temperatures. The last line gives the observed LEED pattern. HW stands for heavy domain wall structure of $\sqrt{3}$ domains.

Temperature (K)	380	460	540
θ_H	0.22	0.0	0.0
θ_{NH}	0.30	0.24	0.0
θ_N	0.17	0.23	0.38
LEED	HW	HW	$\sqrt{3}$

show no desorption of hydrogen. Comparing the spectra of mass 2 and mass 14 we can distinguish three temperature regions, namely,

(I) 380 K$<T<$460 K: only hydrogen desorbs;

(II) 460 K$<T<$540 K: hydrogen and nitrogen desorb with high rate;

(III) 540 K$<T$: only nitrogen desorbs.

The amount of desorbing hydrogen can be estimated by comparing the TDS integrals of mass 2 and mass 28. Taking the different ionization probabilities of N_2 and H_2 into account, the total amount of H_2 that desorbs corresponds to a hydrogen coverage of $\theta_H=0.52\pm0.05$. In region I (II) an amount of H_2 desorbs which is equivalent to $\theta_H=0.28$ (0.24). The hydrogen desorption in region II is accompanied by the desorption of N_2 whose amount corresponds to about $\theta_N=0.1$ (see Table I).

The TD spectrum of mass 2 recorded simultaneously with spectrum d in Fig. 1 shows no hydrogen desorption. Although at a first glance the data of Fig. 3 might suggest that the N_β peak of the N_2 TDS data are limited by decomposition of NH_{ad} rather than by recombination of $2N_{ad}$. The missing H desorption for spectrum d in Fig. 1 clearly indicates that indeed the latter effect is responsible for thermal desorption at higher θ_N. That means mutual repulsion reduces the effective surface bond strength of N_{ad}. However, above $\theta_N=0.38$ this bond has weakened so much that there the N_{ad} species recombine and desorb immediately after formation through dissociation of NH_{ad}.

B. LEED

Figure 4 displays the two different LEED patterns with split adsorbate spots which we found after the preparation sketched in Fig. 2 and some annealing as noted in the following. After annealing the sample to 420 K, we found a $\sqrt{3}$ pattern with split adsorbate spots [Fig. 4(a)]. The $\sqrt{3}$ spots are replaced by equilateral triangles with one spot at every tip. The tips of the triangles point towards the substrate spots. This LEED pattern does not change for annealing temperature $\leqslant$470 K at which the nitrogen desorption starts (Fig. 1). In a series of experiments it was checked that the positions of the split spots do not vary with coverage. We define a relative split by dividing the distance between the split spot and the $\sqrt{3}$ spot by the distance between two nearest-neighbor substrate spots from the substrate. From all taken LEED photographs we derived a relative split of 0.145 ± 0.02.

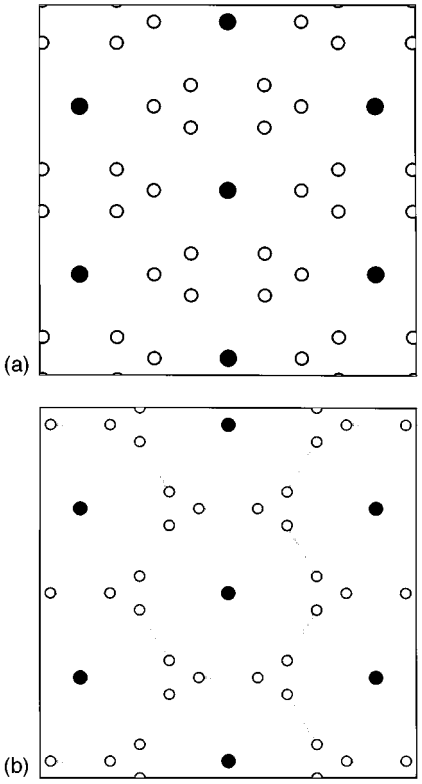

FIG. 4. Schematic sketches of the LEED-patterns observed after the maximum NH_3 dose according to Fig. 2 and annealing to (a) 420–480 K and (b) 540–600 K. The spot positions are calculated according to the models of Figs. 5(a) and 5(b).

Further annealing to 520 K resulted in a sharp, unsplit $\sqrt{3}$ pattern which is not shown here. From the TD spectra in Fig. 1 the nitrogen coverage after this annealing temperature can be determined to $\theta_N=0.34$.

Heating the sample to higher temperatures, the $\sqrt{3}$ spots disappeared, and the LEED pattern, schematically shown in Fig. 4(b), was monitored. This LEED pattern can again be interpreted as a $\sqrt{3}$ pattern with split spots, but, contrary to Fig. 4(a), the tips of the triangles point between the substrate spots. The split spots are streaked towards the 2×2 spots. So, the pattern can also be called a split 2×2 one.

After annealing the sample to 590 K a sharp 2×2 pattern was observed. This LEED pattern was stable up to 630 K. From the TDS measurements we deduce that the coverage after this annealing temperature is $\theta_N=0.26$ which is in good accordance with the coverage of $\theta_N=0.25$ implied by the 2×2 LEED pattern. The same 2×2 LEED pattern could previously be prepared by a high exposure to N_2 ($\sim10^6$ L) at 500 K with the pressure gauge on.[7]

The split $\sqrt{3}$ LEED patterns can be interpreted as due to hexagonal domain structures formed by domains of $\sqrt{3}$ structure with different sizes and different domain walls, namely the $\sqrt{3}$ heavy-wall (HW) [Fig. 5(a)] and the light-wall (LW) domain structures [Fig. 5(b)] as shown by Zeppenfeld *et al.*[14] The NN distance of the nitrogen atoms across the domains walls is 1 in the HW and 2 in the LW both in units of the Ru(0001) lattice. From the split of the $\sqrt{3}$ spots the size and

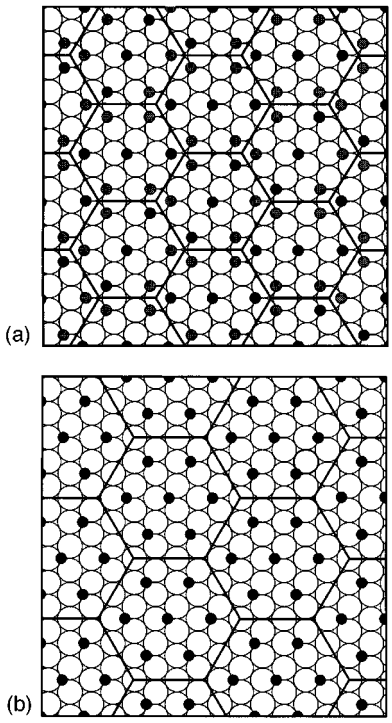

FIG. 5. Schematic sketches of the local structure of the (a) heavy-domain wall $\sqrt{3}$ and (b) 2×2 structure. Large circles, Ru atoms; small circles, adsorbate atoms. The domain walls are indicated as lines.

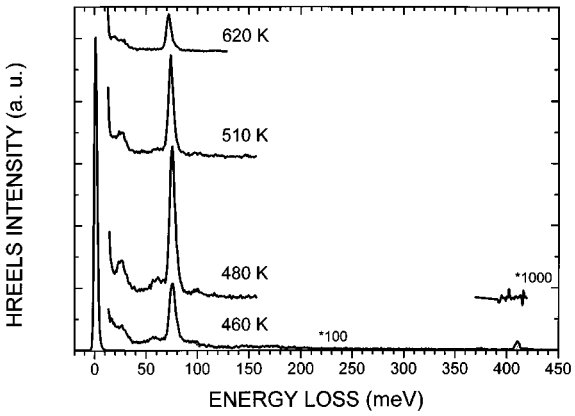

FIG. 6. HREEL spectra for the maximum NH_3 dose according to Fig. 2. After dosing, the sample was subsequently annealed to the indicated temperatures. The primary energy of the electrons was 1.5 eV. All spectra were recorded in specular geometry with an angle of incidence of 60° with respect to the surface normal.

the type of the domain walls can be deduced. Making the reasonable assumption, that N is ordered within a $\sqrt{3}$ structure, the coverage can be determined from the relative split. Table II displays a summary of domain sizes, their relative split and the coverage of these structures. For the $\sqrt{3}$ light-wall domains the smallest density of N can be achieved for domains of size 5 for which $\theta_N=0.28$. For larger $\sqrt{3}$ domains the coverage increases and the relative shift decreases. Therefore, the observed LEED pattern of Fig. 4(b) is better interpreted as a split 2×2 one due to a heavy-wall 2×2 domain structure. As can be seen from Table II, with increasing domain sizes the coverage approaches 0.250. The streaking can be explained as due to a distribution of 2×2 heavy-wall domains of different size. Figure 5 shows schematic distributions of adsorbates in the heavy-wall $\sqrt{3}$ domain [Fig. 5(a)] and in the heavy-wall 2×2 domain [Fig. 5(b)] generating the LEED patterns of Fig. 4.

The split of the heavy-wall $\sqrt{3}$ LEED pattern we monitored indicates a coverage of $\theta_N=0.438$. This value is slightly smaller than the integral coverage of $\theta_N=0.47$ obtained from the TDS measurements. This difference might still be within the limits of accuracy, but it might alternatively reflect the fact that about 6% of the surface is covered by additional 1×1 domains.

C. HREELS

In order to derive informations on the nature of the adsorbed species we employed HREELS. Figure 6 shows the HREEL spectra of a surface exposed to NH_3 by the procedure as described in Fig. 2. The spectrum recorded after annealing to 460 K is, besides some difference in intensity, identical to the spectrum recorded directly after dosing and shows a main loss at 72 meV and three minor losses at 26, 60, and 410 meV. The main loss at 72 meV is due to the known ν(Ru–N) vibration.[13,15] The loss at 410 meV is identified as the ν(N–H) vibration[15,16] and is an indicator for N–H groups on the surface. NH_2 and NH_3 can be excluded since they are always accompanied with other intense losses which are not detected here.[15–17] The ν(Ru–NH) mode, which is expected at 86 meV,[15] is only very weak. It seems generally to be of faint intensity on Ru(0001).[16,18] The δ(NH) mode is not visible indicating that NH is standing in an upright configuration in which this mode is not dipole allowed.[16] After annealing the sample from 470 K to 485 K the intensity of the ν(Ru–N) mode is increased by a factor of

TABLE II. A summary of different heavy and light wall domains and their coverage and relative split. The domain size is given as the distance between two parallel sides of a single domain in units of the Ru next-neighbor distance.

Domain size	HW 2×2	LW $3\sqrt{3}$	LW $5\sqrt{3}$	LW $7\sqrt{3}$	LW $\sqrt{3}$	LW 5	LW 8	LW 11	HW $\sqrt{3}$	HW 4	HW 7	HW 10
Coverage		0.259	0.253	0.252		0.280	0.297	0.301		0.438	0.388	0.370
Relative split		0.121	0.159	0.175		0.115	0.072	0.053		0.144	0.083	0.058

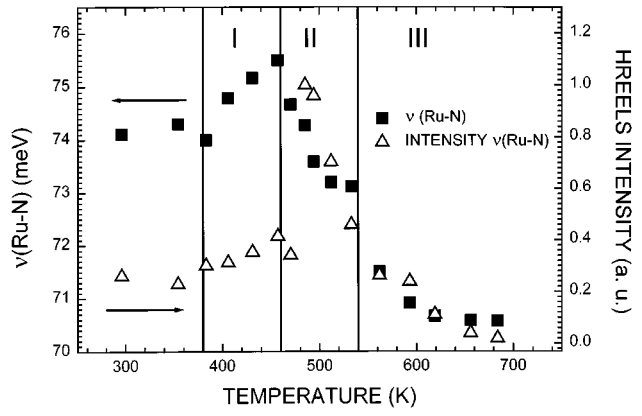

FIG. 7. The energy of the ν(Ru–N) mode and its intensity as a function of annealing temperature.

3. In the same annealing step the ν(N–H) signal disappears completely. At even higher annealing temperatures the ν(Ru–N) vibration loses intensity as shown in Fig. 7.

With the disappearance of NH also the mode at 26 meV gains substantially in intensity. The intensity varies with coverage in the same way as the ν(Ru–N) mode does. Mitchell *et al.*[19] observed two dipole active surface phonon modes at 18 and 29 meV induced by oxygen atoms on Ru(0001). Since both oxygen and nitrogen[20] adsorb in a threefold hollow site and in a very similar geometry, we attribute the loss at 26 meV to a nitrogen induced surface phonon.

Figure 7 shows the HREELS intensity of the ν(Ru–N) vibration together with the frequency of the ν(Ru–N) vibration as a function of annealing temperature. In region I (380 K–460 K) the ν(Ru–N) intensity gains intensity while the ν(N–H) mode loses about 20% intensity. Parallel to the increase in intensity the frequency of the ν(Ru–N) shifts to higher energy; at 460 K the ν(Ru–N) mode reaches its maximum frequency at 75.5 meV. Region II (460 K–540 K) is characterized by the jump of the ν(Ru–N) intensity by factor of 3 after annealing to 485 K. At the same annealing step the ν(N–H) mode disappears completely. Note that the jump does not occur in parallel with the highest ν(Ru–N) frequency at 460 K.

Combining the HREELS with the TDS results we can address the question of the nature of the adsorbed species in the three temperature regions.

1. Region I (380 K<T<460 K)

In region I only hydrogen desorbs. Recently, Seets *et al.*[21] have shown that for a nitrogen coverage of $\theta_N=0.33$ the hydrogen desorption is completed at 320 K. This result underlines that the hydrogen desorption states cannot be due to the coadsorption of H+N alone. From HREELS we know that NH is present on the surface, but HREELS does not give the absolute coverage of NH. In region I we observe a drop of 20% in the ν(N–H) intensity. This implies that the desorbing hydrogen may partly be due to the decomposition of NH. It seems, however, unlikely that the total amount of $\theta_H=0.28$ originates from the dissociation of NH. We rather assume that the main amount of desorbing hydrogen is due to hydrogen coadsorbed with N and NH. Even if hydrogen does not coadsorb in the presence of N this might well be the case with NH species.

2. Region II (460 K<T<540 K)

Region II is characterized by the disappearance of the ν(N–H) mode in the HREEL spectra, accompanied with the jump in the intensity of the ν(Ru–N) mode and the sharp N_β peak in the TD spectra. Obviously NH decomposes in this region, and hydrogen desorbs since it is not stable as a coadsorbate together with nitrogen. Part of the nitrogen coverage also desorbs. At least a part of this N_2 released into the gas phase is independent of the decomposition of NH since in spectrum d we monitor nitrogen desorption which is not accompanied with hydrogen desorption.

3. Region III (540 K<T)

For annealing temperatures exceeding 480 K the intensity of the ν(Ru–N) mode drops continuously as the nitrogen coverage decreases with progressing desorption from the H_α state. The vibrational frequency changes with increasing annealing temperature from 75.5 meV to 70.6 meV at low nitrogen coverage. The dipole moment per adsorbed nitrogen atom was determined by Rauscher *et al.*[16] to 1.06×10^{-32} Asm (0.32 D), which is very similar to the dipole moment of oxygen adsorbed on Ru(0001) (0.29 D). Since dipole moment and adsorption geometry of oxygen and nitrogen[20] are very similar, comparable frequency shifts of the ν(Ru–O) and the ν(Ru–N) modes are expected. Indeed oxygen adsorbed on Ru(0001) shows a shift of 5.8 meV from 66.3 meV at $\theta_O=0.25$ to 71.9 meV at $\theta_O=0.5$.[19,22]

From the observations described above we can deduce the coverages of the different adsorbates and follow the transformation from NH to H and N in the three regions (see Table II). At 380 K a coverage of $\theta_H=0.22$, $\theta_{NH}=0.30$, and $\theta_N=0.17$ is on the surface. Heating the sample to 460 K, 0.28 ML of hydrogen desorbs. This hydrogen originates from the adsorbed hydrogen (0.22 ML) and from decomposing NH (0.06 ML). Further heating to 540 K leads to the desorption of 0.1 ML of nitrogen and 0.24 ML of hydrogen. This means that NH decomposes completely, the hydrogen desorbs, and 0.1 ML of N desorbs also. At 540 K only 0.38 ML of nitrogen are left on the surface.

The jump in the ν(Ru–N) HREELS intensity after annealing to 470 K (see Fig. 6) might suggest that the amount of nitrogen on the surface increases by a factor of about 3. This is not the case and, therefore, not contradictory to the TDS results above, since the HREELS intensity is not necessarily proportional to the coverage. Instead, the coadsorbed NH may well have affected the dynamic dipole moment of the Ru–N complex.

IV. DISCUSSION

First we discuss the maximum N coverage one can achieve on the Ru(0001) surface. With ionization-gauge assisted dissociation of N_2 we have observed a maximum cov-

erage of $\theta_N=0.25$ in accordance with the 2×2 LEED pattern found at 90 K.[7] This value is also in agreement with results from another experiment in which Rosowski *et al.*[10] studied a real Ru catalyst on a MgO support in a flow experiment using a microreactor. Saturation with chemisorbed N was achieved by flowing N_2 at a pressure of 1 bar for 14 h over the catalyst which was held at 573 K. The dose applied in this experiment amounted to 4×10^{13} L. A saturation value of $\theta_N=0.22$ was found. 80% of this value was already attained after 2×10^{12} L. (The value of $\theta_N=0.22$ corresponds to curve b in Fig. 1.) The sample temperature of 573 K was chosen in order to avoid the blocking of surface sites by CO or H. Bulk N does not play a role since the Ru particles are only about 2 nm in diameter so that a large fraction of the Ru atoms is at the surface. From a kinetic modeling of their results Rosowski *et al.*[10] deduced a sticking coefficient of 10^{-14} at 300 K. In an UHV experiment we have recently derived an initial sticking coefficient of $(1\pm0.8)10^{-12}$ at the same temperature.[7] The UHV experiment certainly is at the limit of its feasibility.

In order to prepare N coverages beyond 0.25 we had to use another method which was decomposition of NH_3 in our case. The NH_3 decomposition is well studied[8,9,23,24] and also decomposition at higher temperatures has been used already.[8] Our procedure combines the high decomposition rate at higher temperatures and avoids N_2 desorption by lowering the sample temperature at the end of the decomposition experiment. The maximum coverage of N-containing species is 0.47. This value is in agreement with the value reported by Tsai and Weinberg.[8] The corresponding LEED patterns, however, are completely different: They observe a 2×2 one whereas we observe a split $\sqrt{3}$ structure. We also show here by HREELS and TDS that under these conditions a large part of N is in the form of NH, i.e., the NH_3 decomposition is not completed yet. Our results also show that such a large amount is not stable exclusively as N_{ad}. During decomposition pronounced desorption peaks occur for both N_2 and H_2, i.e., if a coverage of $\theta_N=0.38$ is exceeded through NH decomposition, the surplus N desorbs immediately as N_2. The maximum nitrogen concentration is, however, stable on the surface within a N+NH coadsorbate phase.

An atom model for the occupation of the HW domain in Fig. 5(a) is not quite obvious. The coverage in Fig. 5(a), which can be easily verified by counting the atoms, is 0.44, i.e., somewhat smaller than the value of 0.47 derived from TDS. The relative proportion of NH:N is approximately 5:3 (Table II). In Fig. 5(a) there are only 7 adspecies which might be distributed between NH and N according to 4:3 or 5:2. The density of adsorbed species is very high at the corners of the domains. These triangles might, on the average, be occupied by two NH and one N. However, any further conclusions on the actual structure of this phase would be pure speculation.

After complete decomposition of NH and desorption of hydrogen a value of $\theta_N=0.38$ was achieved. According to Table II it would be possible to model this density by domains of size 7 with heavy walls. We have not observed the equivalent LEED pattern which may indicate that the entropy term wins in this case and that the formation of heavy domain walls was made possible through the stabilization between the N and NH species in the 2NH+1N local trimers at the corners of the domain. A N density larger than $\theta_N=0.33$ indicates that locally N 1×1 domains occur.

At the end of our discussion of the different LEED patterns we mention the work of Rauscher *et al.*[16] which studied the decomposition of hydrazine (N_2H_4) on Ru(0001). At about 450 K, i.e., above the last H_2 desorption peak, when only chemisorbed N is left on the surface, they observed a split $(\sqrt{3}\times\sqrt{3})R$ 30° pattern in LEED with the tips of the triangles pointing between the substrate spots. They derived $\theta_N=0.36$–0.37 for this state and explained the LEED pattern by superheavy domain walls. The maximum θ_N they could prepare is in very good agreement with our result. The split LEED pattern is different, however.

With respect to the HREELS results some remarks have to be made, too. The maximal relative intensity of the ν(Ru–N) mode is 4.7×10^{-3} (Fig. 6) and is found for $\theta_N=0.38$. This is larger than the value of about 2×10^{-3} in our older work,[13] where we used ionization-gauge assisted dissociative adsorption of N_2. This confirms that the coverage in Ref. 13 was 0.25 at maximum.[7] This is also in very good agreement with the Ru–N frequency which we found in this work to shift from 71 meV at $\theta_N\approx0.2$ to 75.5 meV at $\theta_N=0.38$. In Ref. 13 we have observed ν(Ru–N)=71 meV for all coverages achieved at that time. In the light of our recent results and also of ionization-gauge assisted N_2 dissociation on Ru(1010) (Ref. 17) we assign the higher lying losses in Ref. 13 to CH and NH species and not to more loosely bound N. Since N is thought to be adsorbed at a threefold-hollow site similar to O it is interesting to note that the energy shift of the ν(Ru–N) mode to higher energies with coverage is also quite similar. Considering the Ru–N chemical bond the direction of these shifts is not understood yet. With increasing coverage the bond to surface is weakened and the potential normal to the surface gets shallower which should reduce the frequency of the perpendicular motion opposite to the experimental result. The direction of the shift is in accordance with that expected for an anticipated dipole–dipole interaction. The amount of the shift is also in accordance with dipole–dipole interaction at least for Ru–N and neglecting any change in bond strength.

A further point is very remarkable. Although for the lowest curve in Fig. 6 the ratio of NH to N is 5:3 we observe no Ru–NH mode. The existence of NH is well demonstrated by the N–H stretch mode at 410 meV but the expected Ru–NH mode at 86 meV is completely absent. This mode is clearly observed when NH is formed by interaction of N and H.[13] The only explanation we have so far is derived from an analogy to the Cs+CO compound layer. For this system it is found by LEED structure analysis[25] and HREELS (Refs. 26, 27) that the CO–Ru mode is nearly completely suppressed when CO is shifted from the on-top site in the CO/Ru(0001) system to the threefold-hollow site in the (Cs+CO)/Ru(0001) compound system. From this analogy we would conclude that NH is bonded at a threefold-hollow site which

would confirm the heavy wall domain model presented above.

A final remark concerns the maximal density of N which can be achieved on Ru(0001). At this point there is a large difference to oxygen. For O/Ru(0001) it was first speculated[28,29] and recently shown[30] that an oxygen coverage of $\theta_O=1$ can be prepared through dissociation of NO_2. Dissociation of O_2 leads only to $\theta_O=0.5$ due to kinetic limitations. For N/Ru(0001) the situation is different. First, with direct, ionization-gauge assisted, dissociation a coverage of about $\theta_N=0.25$ can be achieved only. Furthermore, we have observed in this study that, although there is $\theta_N=0.47$ in the (N+NH) compound layer, only a coverage of $\theta_N=0.38$ is kept on the surface during decomposition of NH. One may speculate, however, that the N coverage may be increased if one would be able to bring more atomic N onto the surface at lower surface temperatures.

V. CONCLUSIONS

Using a special procedure for the decomposition of NH_3 on Ru(0001) a maximum nitrogen coverage of $\theta_N=0.38$ can be prepared which shows desorption maxima at 540 and 680 K in TDS. For $\theta_N=0.33$ a sharp $\sqrt{3}$ pattern is observed. With decreasing θ_N it turns into a split 2×2 (due to 2×2 domains with heavy domain walls) and then into a 2×2 pattern.

If the sample temperature during NH_3 decomposition is held at 350 K, H, NH, and N are adsorbed in a composite layer. In this layer NH stabilizes both H and N to such an extent that coverages of $\theta_{(H+NH)}=0.52$ and $\theta_{(N+NH)}=0.47$ are stored at the surface. This composite phase exhibits a split-$\sqrt{3}$ LEED pattern which can be attributed to a heavy wall $\sqrt{3}$ domain structure of diameter 4. With increasing temperature first H_2 is desorbed and then H_2+N_2, the latter within a sharp first-order type desorption process at 500 K. The latter process is shown to consist of a dissociation of NH and a break down of the N+NH compound layer which leads to a spontaneous desorption of H_2 and N_2. Atomic nitrogen with $\theta_N>0.38$ is not stable at 500 K. So far no process is known to increase the N coverage beyond 0.38. From the analogy with oxygen one may speculate that it may be larger for temperatures below 500 K.

The energy of the ν(Ru–N) mode shifts from 70.6 to 75.5 meV, i.e., to higher energies by about 5 meV when the coverage is increased from 0.25 to 0.38 similarly as with the O–Ru(0001) system. A N-derived phonon is observed at 26 meV. In the N+NH compound the Ru–NH mode shows nearly no intensity. In analogy to the (Cs+2CO) Ru(0001) (2×2) system it is concluded that NH is adsorbed at a threefold-hollow site which seems to completely screen any Ru–NH dipole moment.

ACKNOWLEDGMENTS

We are grateful to M. Muhler for stimulating discussions. We thank P. Geng for dedicated technical support and M. Richard for typesetting the manuscript.

[1] A. Ozaki and K. Aika, in *Catalysis-Science and Technology*, edited by J. R. Anderson and M. Boudart (Springer, Berlin, 1981), Vol. 1, p. 87.
[2] G. Ertl, *Catalytic Ammonia Synthesis* (Plenum, New York, 1991), p. 109.
[3] K.-I. Aika and K. Tamaru, *Ammonia Catalysis and Manufacture* (Springer, Berlin, 1995), p. 103.
[4] S. R. Tennison, *Catalytic Ammonia Synthesis* (Plenum, New York, 1991), p. 303.
[5] J. Parmeter, Y. Wang, C. Mullins, and W. Weinberg, J. Chem. Phys. **88**, 5225 (1988).
[6] Y. Zhou, S. Akhter, and J. E. White, Surf. Sci. **202**, 357 (1988).
[7] H. Dietrich, P. Geng, K. Jacobi, and G. Ertl, J. Chem. Phys. **104**, 375 (1996).
[8] W. Tsai and H. Weinberg, J. Chem. Phys. **91**, 5302 (1987).
[9] C. Egawa, T. Nishida, S. Naito, and K. Tamaru, J. Chem. Soc. Faraday Trans. I **80**, 1595 (1984).
[10] F. Rosowski, O. Hinrichsen, M. Muhler, and G. Ertl, Catal. Lett. **36**, 229 (1996).
[11] H. Ibach, *Electron Energy Loss Spectrometers—The Technology of High Performance* (Springer, Berlin, 1991).
[12] H. Pfnür, P. Feulner, and D. Menzel, J. Chem. Phys. **79**, 161 (1983).
[13] H. Shi, K. Jacobi, and G. Ertl, J. Chem. Phys. **99**, 9248 (1993).
[14] P. Zeppenfeld, K. Kern, R. David, and G. Comsa, Phys. Rev. B **38**, 3918 (1988).
[15] H. Shi, K. Jacobi, and G. Ertl, J. Chem. Phys. **102**, 1432 (1995).
[16] H. Rauscher, K. Kostov, and G. Menzel, J. Chem. Phys. **177**, 473 (1993).
[17] H. Dietrich, K. Jacobi, and G. Ertl, Surf. Sci. **352-354**, 138 (1996).
[18] J. Parmeter, U. Schwalke, and W. Weinberg, J. Am. Chem. Soc. **110**, 53 (1988).
[19] W. J. Mitchell, Y. Wang, M. Schick, and W. H. Weinberg, J. Chem. Phys. **102**, 8185 (1995).
[20] S. Schwegmann, H. Dietrich, H. Over, K. Jacobi, A. Seitsonen, M. Scheffler, and G. Ertl, Surf. Sci. (to be published).
[21] D. C. Seets, M. C. Wheeler, and C. B. Mullins, J. Chem. Phys. **103**, 10 399 (1995).
[22] T. S. Rahman, A. B. Anton, N. R. Avery, and W. H. Weinberg, Phys. Rev. Lett. **51**, 1979 (1983).
[23] C. Egawa, S. Naito, and K. Tamaru, Surf. Sci. **125**, 605 (1983).
[24] C. Egawa, S. Naito, and K. Tamaru, Surf. Sci. **138**, 279 (1984).
[25] H. Over, H. Bludau, R. Kose, and G. Ertl, Phys. Rev. B **51**, 4661 (1995).
[26] K. Jacobi, H. Shi, M. Gruyters, and G. Ertl, Phys. Rev. B **49**, 5733 (1994).
[27] P. He, Y. Xu, and K. Jacobi, J. Chem. Phys. **104**, 8118 (1996).
[28] C. H. F. Peden and D. W. Goodman, J. Phys. Chem. **90**, 1360 (1986).
[29] C. H. F. Peden and D. W. Goodman, Surf. Sci. **253**, 44 (1991).
[30] C. Stampfl, S. Schwegmann, H. Over, M. Scheffler, and G. Ertl, Phys. Rev. Lett. (in press).